Cukurova University
Journal of
Natural & Applied Sciences

Original Paper

Analytical Solutions of Two-dimensional Solute Transport with Spatially and Temporarily Dependent Dispersion in Heterogeneous Porous Media

Raja Ram YADAV[1], Sujata KUSHWAHA[1], Joy ROY[2]

[1]Department of Mathematics and Astronomy, University of Lucknow, Lucknow 226007- India
[2]Department of Mathematics, Aryavart Institute of Higher Education, Lucknow 226025- India

ORCID IDs of the authors: R.R.Y. 0000-0002-1311-5435; S.K. 0000-0003-0467-3862; J.R. 0000-0003-0403-3048.

Cite this article as: Yadav, R, R., Kushwaha, S., Roy, J. (2023). Analytical Solutions of Two-dimensional Solute Transport with Spatially and Temporarily Dependent Dispersion in Heterogeneous Porous Media. Cukurova University Journal of Natural & Applied Sciences 2(2): 17-36.

Abstract

The aim of this study is to develop a two-dimensional mathematical model for the conservative solute transport in heterogeneous adsorbing porous media. Solutions for semi-infinite and finite domains are obtained in two separate cases. Groundwater velocity is considered to be a linear function of position as well as a function of time. After a certain time interval, the velocity of the groundwater changes over different time periods, so mathematically it is represented by a different temporarily dependent function. The dispersion coefficient is squarely proportional to groundwater velocity with position in both directions and directly proportional to time. Space and time-dependent groundwater velocity and dispersion coefficients are assumed to be in degenerate forms. The assumption of segmented, temporally, and spatially correlated diffusion and groundwater velocities is a unique feature of this paper. The input source applied along the flow is of uniform nature. The concentration gradient along both axes is set to zero at non-source end of both semi-infinite and finite domain cases. The Laplace Integral Transform Technique (LITT) is used to obtain the final solution to the proposed problem. The effect of aquifer heterogeneity and spatio-temporal dependence of dispersion on the solute transport is shown graphically in each case.

Keywords: Advection, Dispersion, Groundwater velocity, Heterogeneity, Porous media.

1. Introduction

The transport of solutes is a significant physical phenomenon that usually occurs through porous media in a variety of industrial, natural, and non-natural systems. Understanding the process of solute transport is a challenging task due to the complex structure of porous media. Structurally, most of the porous media that exist in the subsurface are heterogeneous in nature. At different length scales, the spatial distribution of heterogeneity can have a significant impact on aquifer dynamics as well as flow behavior. Waste on the earth's surface seeps into the groundwater through rainwater, thereby polluting the groundwater. The groundwater gets polluted due to the seepage of waste accumulated on the earth's surface through rainwater. An efficient mathematical model helps us understand solute transport phenomena, although it is difficult to develop due to complex geological conditions. A mathematical model, that describes the processes of groundwater flow and solute transport in porous media, is represented by the advection-dispersion equation (ADE). In addition to hydrodynamic conditions, dispersion, groundwater velocity, retardation factors, and solute properties also influence the solute transport process. In the literature, there are many approaches to address problems of contamination mixing in groundwater in form of one- or two- or three-dimensional studies. Over the past few decades, many researchers have studied the effects of pollutant transport in aquifer systems based on common assumptions like unsteady velocity, homogeneous porous medium [1-2]. Many researchers have attempted to characterize the effects of transient conditions on the transport of pollutants in aquatic systems. In the past, many researchers have solved time-varying models using analytical and numerical techniques [3-4]. It is an established fact that variations in the direction of the hydraulic gradient are more important than variations in its magnitude [5]. Batu [6-7] used Fourier analysis and the Laplace transform to develop a two-dimensional analytical solution for solute transport in a bounded aquifer. Broadbridge et al. [8] obtained an analytical solution for velocity-dependent dispersion in two-dimensional isotropic porous media. Chen et al. [9] developed an analytical solution for a two-dimensional ADE with linearly spatially dependent dispersion using a power chain method. Yadav et al. [10] developed an

Address for Correspondence:
Joy Roy, e-mail: joyroy2904@gmail.com

Received: Feb 23, 2023
Accepted: Jun 21, 2023

analytical solution for the two-dimensional additive-diffusion equation in isotropic finite porous media using the Laplace Integral Transform Technique.

Analytical solutions to the two-dimensional advection-dispersion equation in porous media were developed using the Laplace Integral Transform Technique [11]. Singh and Mahato [12] proposed solution for two-dimensional transport problem for accessing the effect of dispersion on distribution of the concentration generated from a time dependent input sources. Singh et al. [13] obtained solution for transport problem considering varying pulse-type stationary point source in two-dimensional flow to examine the role of different parameters. Singh and Ahamad [14] presented solution of one-dimensional transport problem to state the effect of temporal dispersion and groundwater velocity on solute distribution with time and position. Perez Guerrero et al. [15] used the Generalized Integral Transform Technique (GITT) to develop a formal exact solution to the linear advection-dispersion equation with transient and constant coefficients. It is well known that the spatial pattern, composition, and heterogeneity of media play a significant impact in determining solute transport [16-17]. Chen et al. [18] obtained analytical solutions to the two-dimensional advection-dispersion equations (ADE) in cylindrical coordinates using Laplace and Finite Hankel transform techniques under third type of input boundary condition. Singh et al. [19] established an analytical solution for two-dimensional solute transport in a finite homogeneous aquifer using the Hankel transform technique. In a finite porous media domain, Chen et al. [20] developed an analytical solution for two-dimensional solute transport in a cylindrical coordinate system. The two-dimensional linear advection-dispersion equations in cylindrical coordinates over a finite domain are obtained analytically under the first and third kinds of boundary conditions [4].

The purpose of this study is to develop a comprehensive analytical solution for the transport of solutes in two-dimensional semi-infinite and finite heterogeneous porous media. Two key parameters (dispersion and groundwater velocity) are considered in degenerate form. Furthermore, for different time intervals, the dispersion coefficient and groundwater velocity are considered to be different smooth functions of time. The closed-form analytical solutions of the two-dimensional advection-dispersion equation (ADE) are obtained using the Laplace Integral Transform Technique. Finally, the analytical solutions illustrated graphically with the help of appropriate input parameters. The developed model can objectively assess pollution levels in any given situation and time, and this information can help the government authorities to take remedial measures.

2. Mathematical Formulation and Solution of the Problem

This study describes the two-dimensional non-reactive solute transport in a semi-infinite heterogeneous porous medium to predict the concentration in the domain. The governing two-dimensional advection-dispersion equation (ADE) describing the solute transport in adsorbing porous medium may be written as:

$$R\frac{\partial c}{\partial t}=\frac{\partial}{\partial x}\left\{D_{xx}\frac{\partial c}{\partial x}+D_{xy}\frac{\partial c}{\partial y}-u_x c\right\}+\frac{\partial}{\partial y}\left\{D_{yy}\frac{\partial c}{\partial y}+D_{yx}\frac{\partial c}{\partial x}-u_y c\right\} \tag{1}$$

where $c(x,y,t)$ $[ML^{-3}]$ is the contaminant concentration, x $[L]$ and y $[L]$ are the longitudinal and transverse coordinates, respectively and t $[T]$ is time, D_{xx} $[L^2T^{-1}]$, D_{yy} $[L^2T^{-1}]$, D_{xy} $[L^2T^{-1}]$ and D_{yx} $[L^2T^{-1}]$ are components of two-dimensional dispersion coefficients tensor [21]. u_x $[LT^{-1}]$ and u_y $[LT^{-1}]$ are components of groundwater velocity in directions of coordinate x and y axes, respectively. The governing equation also includes the retardation factor R which is a dimensionless quantity occurs in the porous medium due to adsorption. There are three important mechanisms for solute transport in porous media: diffusion, dispersion and convection. The effect of diffusion is considered to be negligible. Groundwater velocity and dispersion coefficient are spatially and temporally dependent, and their nature changes after a certain period of time. Expressions of space-time dispersion coefficient and groundwater velocity along x and y directions are expressed as:

$$u_h=u_{h0}(1+z_h)F(t) \text{ and } D_{gh}=D_{gh0}(1+z_g)(1+z_h)F(t); \tag{2}$$

where, $F(t)=\begin{cases} f_1(m_1t); 0<t\le t_1 \\ f_2(m_2t); t_1<t\le t_2 \\ f_3(m_3t); t_2<t \end{cases}$; $g=x,y$; $h=x,y$; $z_x=ax$ and $z_y=by$. Also $D_{xy0}=D_{yx0}$.

Substituting Eq. (2) in Eq. (1) we get;

$$R\frac{\partial c}{\partial t}=\frac{\partial}{\partial x}\left\{D_{xx0}\left(1+ax\right)^2F(t)\frac{\partial c}{\partial x}+D_{xy0}\left(1+ax\right)\left(1+by\right)F(t)\frac{\partial c}{\partial y}-u_{x0}\left(1+ax\right)F(t)c\right\}+$$
$$\frac{\partial}{\partial y}\left\{D_{yy0}\left(1+by\right)^2F(t)\frac{\partial c}{\partial y}+D_{xy0}\left(1+ax\right)\left(1+by\right)F(t)\frac{\partial c}{\partial x}-u_{y0}\left(1+by\right)F(t)c\right\} \quad (3)$$

where, D_{xx0}, D_{yy0} and u_{x0}, u_{y0} are initial values of the corresponding dispersion coefficients and groundwater velocity along x and y axes, respectively. The expression $f_i\left(m_i t\right); i=1,2,3$ is dimensionless and m_i is an unsteady parameter having dimension inverse of time. a and b are the heterogeneity parameter having dimension inverse of position. The study of semi-infinite and finite domain heterogeneous porous media is carried out in two different scenarios of case 1 and case II, respectively. It's worth noting that the only fundamental difference between the two cases is the length of the porous domain. The comparative study gives us a better opportunity to understand the effect of the parameters on the distribution pattern of concentration when the size of the domain changes. The cases are as follows:

Case I: For Semi-Infinite Porous Domain

To solve the proposed problem, we assume the following initial and boundary conditions as:

$$c\left(x,y,t\right)=c_i;\ 0\le x<\infty, 0\le y<\infty, t=0 \quad (4)$$

$$c\left(x,y,t\right)=c_0;\ \ x=0, y=0, t>0 \quad (5)$$

$$\frac{\partial c\left(x,y,t\right)}{\partial x}=0;\frac{\partial c\left(x,y,t\right)}{\partial y}=0\ ;\ x\to\infty,\ y\to\infty\ ,t\ge 0 \quad (6)$$

Initially, some concentration c_i [ML^{-3}] is already present in the aquifer. The constant solute source of potential c_0 [ML^{-3}] placed at the point $(0,0)$. The zero flux boundary conditions at the far end/non-source end i.e., at $x\to\infty,\ y\to\infty$ are considered along both axes. Mathematically, these are expressed by Eqs. (3-6).

In order to remove the time-dependent coefficient from Eq. (3), we introduce a new time variable as follows (Crank, 1975) [22]:

$$T=\int_0^t F(t)dt=\int_0^{t_1} f_1\left(m_1t\right)dt+\int_{t_1}^{t_2} f_2\left(m_2t\right)dt+\int_{t_2}^{t} f_3\left(m_3t\right)dt \quad (7)$$

To get the solution in a simple way, we use some suitable transformations.

Using transformation Eq. (7) into Eq. (3) we have:

$$R\frac{\partial c}{\partial t}=\frac{\partial}{\partial x}\left\{D_{xx0}\left(1+ax\right)^2F(t)\frac{\partial c}{\partial x}+D_{xy0}\left(1+ax\right)\left(1+by\right)F(t)\frac{\partial c}{\partial y}-u_{x0}\left(1+ax\right)F(t)c\right\}+$$
$$\frac{\partial}{\partial y}\left\{D_{yy0}\left(1+by\right)^2F(t)\frac{\partial c}{\partial y}+D_{yx0}\left(1+ax\right)\left(1+by\right)F(t)\frac{\partial c}{\partial x}-u_{y0}\left(1+by\right)F(t)c\right\} \quad (8)$$

Using Eq. (7) corresponding initial and boundary conditions Esq. (4-6) may be written in new time variable as follows:

$$c\left(x,y,T\right)=c_i\ ;\ \ 0\le x<\infty, 0\le y<\infty, T=0 \quad (9)$$

$$c\left(x,y,T\right)=c_0\ ;\ \ x=0, y=0, T>0 \quad (10)$$

$$\frac{\partial c(x,y,T)}{\partial x}=0;\frac{\partial c(x,y,T)}{\partial y}=0;x\to\infty,y\to\infty,T\geq 0 \tag{11}$$

To convert the variable coefficient from Eq. (8) to a constant coefficient, we introduce another transformation as follows (Kumar *et al.*, 2010) [23]:

$$X=\int_0^x\frac{1}{(1+ax)}dx\ ,Y=\int_0^y\frac{1}{(1+by)}dy\quad \text{or } X=\frac{1}{a}\log(1+ax),\ Y=\frac{1}{b}\log(1+by) \tag{12}$$

Inserting the transformation Eq. (12), Eq. (8) may be written as follows:

$$R\frac{\partial c}{\partial T}=\left(D_{xx0}+D_{xy0}\right)\frac{\partial^2 c}{\partial X^2}+\left(D_{yy0}+D_{xy0}\right)\frac{\partial^2 c}{\partial Y^2}-\left(u_{x0}-D_{xx0}a-D_{xy0}a\right)\frac{\partial c}{\partial X}-\left(u_{y0}-D_{yy0}b-D_{xy0}b\right)\frac{\partial c}{\partial Y}-u_{x0}ac-u_{y0}bc \tag{13}$$

In order to reduce the Eq. (13) into a single position variable z , we use the following transformation as follows:

$$z=X+Y \tag{14}$$

Incorporating the transformation Eq. (14), Eq. (13) reduces as follows:

$$R\frac{\partial c}{\partial T}=\left(D_{xx0}+2D_{xy0}+D_{yy0}\right)\frac{\partial^2 c}{\partial z^2}-\left(u_{x0}+u_{y0}-D_{xx0}a-D_{xy0}a-D_{yy0}b-D_{xy0}b\right)\frac{\partial c}{\partial z}-\left(u_{x0}a+u_{y0}b\right)c \tag{15}$$

Or $$R\frac{\partial c}{\partial T}=D_0\frac{\partial^2 c}{\partial z^2}-U_0\frac{\partial c}{\partial z}-\mu_0 c \tag{16}$$

where, $D_0=D_{xx0}+2D_{xy0}+D_{yy0}$,

$$\left.\begin{aligned}U_0&=u_{x0}+u_{y0}-D_{xx0}a-D_{xy0}a-D_{yy0}b-D_{xy0}b\\ \mu_0&=u_{x0}a+u_{y0}b\ ,\end{aligned}\right\} \tag{17}$$

Using transformations in Eq. (12) and Eq. (14), the corresponding initial and boundary conditions Eqs. (9-11) may be written as follows**:**

$$c(z,T)=c_i\ ;T=0,0\leq z<\infty \tag{18}$$

$$c(z,T)=c_0\ ;T>0,z=0 \tag{19}$$

$$\frac{\partial c(z,T)}{\partial z}=0\ ;\ T\geq 0\ ,z\to\infty \tag{20}$$

We now introduce another transformation to reduce the convective term from Eq. (16) as follows:

$$c(z,T)=k(z,T)\exp\left[\frac{U_0}{2D_0}z-\frac{1}{R}\left(\frac{{U_0}^2}{4D_0}+\mu_0\right)T\right] \tag{21}$$

Inserting the transformation Eq. (21) in Eq. (16) and Eqs. (18-20), we get a diffusive problem in new dependent variable as follows:

$$R\frac{\partial k}{\partial T}=D_0\frac{\partial^2 k}{\partial z^2} \tag{22}$$

$$k(z,T)=c_i\exp(-\beta z);\ z\geq 0, T=0 \tag{23}$$

$$k(z,T)=c_0\exp\left(\eta^2 T\right);\ z=0,\ T>0 \tag{24}$$

$$\frac{\partial k(z,T)}{\partial z}+\frac{U_0}{2D_0}k(z,T)=0;\ z\to\infty\ T\geq 0 \tag{25}$$

where, $\eta=\sqrt{\frac{1}{R}\left(\frac{{U_0}^2}{4D_0}+\mu_0\right)}$ and $\beta=\frac{U_0}{2D_0}$

Now, applying Laplace Integral Transformation, Esq. (22–25) reduce as follows:

$$\frac{d^2\bar{k}(z,p)}{dz^2}-\frac{pR}{D_0}\bar{k}(z,p)=-\frac{R}{D_0}\left\{c_i\exp(-\beta z)\right\} \tag{26}$$

$$\bar{k}(z,p)=c_0\frac{1}{(p-\eta^2)};\ z=0 \tag{27}$$

$$\frac{d\bar{k}(z,p)}{dz}+\frac{U_0}{2D_0}\bar{k}(z,p)=0;\qquad z\to\infty \tag{28}$$

where, p is a Laplace parameter. The solution of Eqs. (26-28) may be written as follows:

$$\bar{k}(z,p)=\frac{c_0}{(p-\eta^2)}\exp\left(-\sqrt{\frac{pR}{D_0}}z\right)-\frac{c_i}{\left(p-\frac{D_0}{R}\beta^2\right)}\times\exp\left(-\sqrt{\frac{pR}{D_0}}z\right)+\frac{c_i\exp(-\beta z)}{\left(p-\frac{D_0}{R}\beta^2\right)} \tag{29}$$

Taking the inverse Laplace Integral Transform to the Eq. (29) and using back transformation Eq. (21), the final solution may be written as follows:

$$c(z,T)=\left[c_0F_\eta(z,T)-c_iF_\rho(z,T)+c_iG_\rho(x,T)\right]\times\exp\left\{\frac{U_0}{2D_0}z-\frac{1}{R}\left(\frac{{U_0}^2}{4D_0}+\mu_0\right)T\right\} \tag{30}$$

where,

$$F_{\phi}(z,T)=\frac{1}{2}\left[\exp\left\{\phi^2 T-\frac{\phi\sqrt{R}z}{\sqrt{D_0}}\right\}erfc\left\{\frac{z\sqrt{R}}{2\sqrt{D_0 T}}-\phi\sqrt{T}\right\}+\exp\left\{\phi^2 T+\frac{\phi\sqrt{R}z}{\sqrt{D_0}}\right\}\right.$$

$$\left.erfc\left\{\frac{z\sqrt{R}}{2\sqrt{D_0 T}}+\phi\sqrt{T}\right\}\right];$$

$$G_{\rho}(z,T)=\exp\left(\rho^2 T-\beta z\right);$$

The values of $F_{\eta}(z,T)$ and $F_{\rho}(z,T)$ are obtained by replacing $\phi=\eta$ and $\phi=\rho$ in $F_{\phi}(z,T)$, respectively.

Case II: For Finite Porous Domain

In this case, the length of the porous domain is finite, and all the initial and boundary conditions are same as taken in Eqs.(4-6) in previous case but are taken for finite domain of length L_1 and L_2 along x and y axes, respectively. These conditions may be written as:

$$c(x,y,t)=c_i\ ;\ 0\le x\le L_1, 0\le y\le L_2, t=0 \tag{31}$$

$$c(x,y,t)=c_0\ ;\ x=0, y=0, t>0 \tag{32}$$

$$\frac{\partial c(x,y,t)}{\partial x}=0;\frac{\partial c(x,y,t)}{\partial y}=0\ ;\ x=L_1;\ y=L_2;\ t\ge 0 \tag{33}$$

where L_1 and L_2 are the longitudinal and transversal length of the porous domain, respectively.

Using Eq. (7), Eqs. (31-33) may be written as follows:

$$c(x,y,T)=c_i\ ;\ 0\le x\le L_1, 0\le y\le L_2, T=0 \tag{34}$$

$$c(x,y,T)=c_0\ ;\ x=0, y=0, T>0 \tag{35}$$

$$\frac{\partial c(x,y,T)}{\partial x}=0;\frac{\partial c(x,y,T)}{\partial y}=0, x=L_1;\ y=L_2, T\ge 0 \tag{36}$$

Using transformation in Eq. (12) and Eq. (14), the initial and boundary condition Eqs. (34-36) may be written as follows**:**

$$c(z,T)=c_i\ ;\ T=0,\ 0\le z\le L \tag{37}$$

$$c(z,T)=c_0\ ;\ T>0,\ z=0 \tag{38}$$

$$\frac{\partial c(z,T)}{\partial z}=0\ ;\ z=L\ ,T\ge 0 \tag{39}$$

where $L=\frac{1}{a}\log(1+aL_1)+\frac{1}{b}\log(1+bL_2)$

Like the differential Eq. (26) obtained by applying Laplace Transformation on Eq. (22) using Eq. (23). The General solution of differential equation which is obtained by applying Laplace Transformation on Eq. (22) using initial condition obtained from Eq. (37) after applying Eq. (21) may be written as follows:

$$\bar{k}(z,p) = C_1 \cosh(Mz) + C_2 \sinh(Mz) + \frac{c_i \exp(-\beta z)}{(p-\rho^2)} \tag{40}$$

And boundary conditions takes Eqs. (37-39) takes the following form after using conditions in Eq. (21) and then taking Laplace Transform Technique as follows:

$$\bar{k}(z,p) = c_0 \frac{1}{(p-\eta^2)}; \quad z = 0 \tag{41}$$

$$\frac{d\bar{k}}{dz} + \frac{U_0}{2D_0}\bar{k} = 0 \; ; \quad z = L \tag{42}$$

Solving the Eq. (40) with boundary conditions the Eqs. (41-42), we have following solution:

$$\bar{k}(z,p) = \left\{ \frac{c_0}{(p-\eta^2)} - \frac{c_i}{(p-\rho^2)} \right\} \frac{M\cosh\{M(z-L)\} + \beta\sinh\{M(L-z)\}}{M\cosh(ML) + \beta\sinh(ML)} + \frac{c_i \exp(-\beta z)}{(p-\rho^2)} \tag{43}$$

where, $M = \sqrt{\frac{pR}{D_0}}$ and $\rho = \sqrt{\frac{D_0}{R}\beta^2}$

Taking Inverse Laplace Transforms Technique of Eq. (43) and using Eq. (21) final solution of present case may be written as follows:

$$c(z,T) = \left[\begin{array}{l} c_0 \left\{ E_1 \exp(\eta^2 T) - 2D_0 L \sum_{n=1}^{\infty} {\omega_n}^2 E_{21} \exp\left(-\frac{{\omega_n}^2 D_0}{RL^2} T \right) \right\} - \\ c_i \left\{ E_3 \exp(\rho^2 T) - 2D_0 L \sum_{n=1}^{\infty} {\omega_n}^2 E_{23} \exp\left(-\frac{{\omega_n}^2 D_0}{RL^2} T \right) \right\} + c_i \exp(\rho^2 T - \beta z) \end{array} \right] \times \exp\left[\frac{U_0}{2D_0} z - \frac{1}{R}\left(\frac{{U_0}^2}{4D_0} + \mu_0 \right) T \right] \tag{44}$$

where

$$E_1 = \frac{G_1}{G_2}; \; E_{21} = \frac{G_3}{G_4}; \; E_3 = \frac{G_5}{G_6}; \; E_{23} = \frac{G_3}{G_7};$$

and

$$G_1 = \gamma\cosh\{\gamma(L-z)\} + \beta\sinh\{\gamma(L-z)\},$$

$$G_2 = \gamma\cosh(\gamma L) + \beta\sinh(\gamma L),$$

$$G_3 = \frac{\omega_n}{L}\cosh\left\{\frac{\omega_n(L-z)}{L}\right\} + \beta\sinh\left\{\frac{\omega_n(L-z)}{L}\right\},$$

$$G_4 = \left(\omega_n{}^2 D_0 + \eta^2 RL^2\right)\left\{\left(\omega_n{}^2 + \beta^2 L^2\right) + \beta L\right\}\sin(\omega_n)$$

$$G_5 = \phi\cosh\{\phi(L-z)\} + \beta\sinh\{\phi(L-z)\},$$

$$G_6 = \phi\cosh(\phi L) + \beta\sinh(\phi L),$$

$$G_7 = \left(\omega_n{}^2 D_0 + \rho^2 RL^2\right)\left\{\left(\omega_n{}^2 + \beta^2 L^2\right) + \beta L\right\}\sin(\omega_n)$$

where, ω_n is the positive root of $\omega_n \cot(\omega_n) + \beta L = 0$

Also $\gamma = \eta\sqrt{R/D_0}$ and $\phi = \rho\sqrt{R/D_0}$

3. Result and Discussion

In this study, a two-dimensional spatially and temporally dependent dispersion model is developed for non-reactive solute transport in two different scenarios (semi-infinite and finite). For semi-infinite and finite domains, the analytical solutions are described by Eq. 30 and Eq. 44, respectively. Different graphs describe the effect of various parameters on the concentration distribution. The value of $L_1 = 0.512$ and $L_2 = 0.512$ are taken for finite domain. For both types (semi-infinite and finite) the longitudinal and lateral domains are taken $0 \le x(km) \le 0.512$ and $0 \le y(km) \le 0.512$ respectively.

For both semi-infinite (Case I) and finite domain (Cases II), the value of the input parameter is chosen as:

The numerical values of the dispersion coefficient and groundwater velocity are derived from the expressions given by Eq. (2).

where,

$$F(t) = \begin{cases} \exp(m_1 t); & 0 < t\,(year) \le 1 \\ s_1 \exp\{m_2(t-1)\} + s_2; & 1 < t(year) \le 5 \\ s_3 \dfrac{m_3(t-5)}{m_3(t-5)+1} + s_4; & t(year) > 5 \end{cases} \quad (45)$$

Components of groundwater velocity along x (longitudinal) and y (lateral) axes are $u_{x_0} = 0.02\left(km\ year^{-1}\right)$, $u_{y_0} = 0.005\left(km\ year^{-1}\right)$, respectively. Reference concentrations are $c_0 = 1$, $c_i = 0.1$. The other regulating parameters are $m_1 = 0.1\left(year^{-1}\right)$, $m_2 = 0.3\left(year^{-1}\right)$ and $m_3 = 0.4\left(year^{-1}\right)$. Retardation factor is $R = 1.25$, and the values of some constants in Eq.(45) are $s_1 = 0.36839$, $s_2 = 0.736781$ $s_3 = 0.917324$ and $s_4 = 1.9598795012568466$.

Case I: For Semi-Infinite Porous Domain

Figs. 1a, 1b, 1c, and 1d are drawn for a semi-infinite porous medium. Fig.1a is the surface plot in xy-plane while Figs. 1b, 1c, and 1d are contour plots drawn for three different times $t = 0.5,\ 2.0, 5.5\,(year)$, respectively and values for dispersion coefficients $D_{xx0} = 0.06\ \left(km^2\,year^{-1}\right)$, $D_{yy0} = 0.04\ \left(km^2\,year^{-1}\right)$ and $D_{xy0} = 0.0053\ \left(km^2\,year^{-1}\right)$ and heterogeneity parameters $a = 0.1\left(km^{-1}\right)$ and $b = 0.1\left(km^{-1}\right)$ are taken for all these graphs (Figs. 1a, 1b, 1c, and 1d).

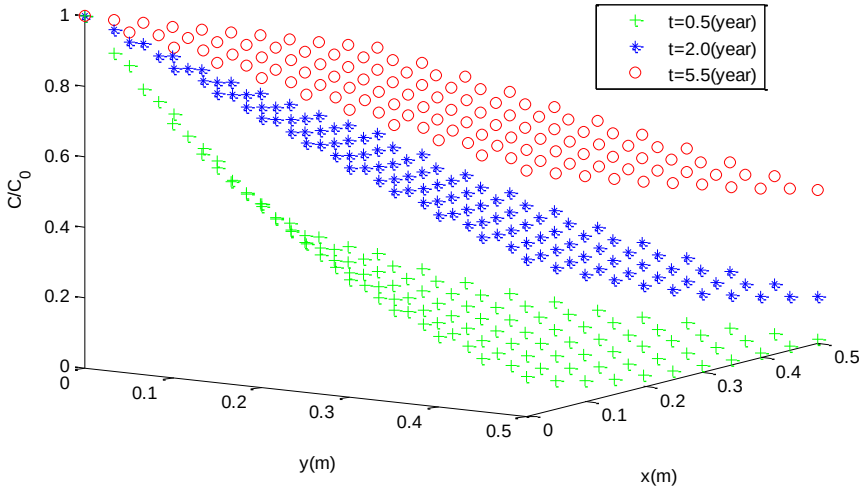

Figure 1a. Surface graph for the concentration profiles obtained from Eq. (30) in three different times period $t = 0.5\,(year)$, $t = 2.0\,(year)$ and $t = 5.5\,(year)$.

Fig.1a explores the concentration profiles at different times in the three time domains $0 < t\,(year) \le 1$, $1 < t\,(year) \le 5$ and $t\,(year) > 5$, respectively, in the square space domain $0 < x\,(km) \le 0.512$ and $0 < y\,(km) \le 0.512$. Concentration levels within the domains were found to increase with time, as groundwater velocity and dispersion coefficients varied with time across all time domains, as shown in Eq. (45). In the first two time domains, the dispersion coefficient and groundwater velocity increase over time, with the effect that the increase in concentration in the first domain is slower than in the second domain. On the other hand, in the last time domain, the concentration value increases asymptomatically. Unlike previous studies, the dispersion coefficient varies over time intervals because the properties of flow may not always remain the same in real situations.

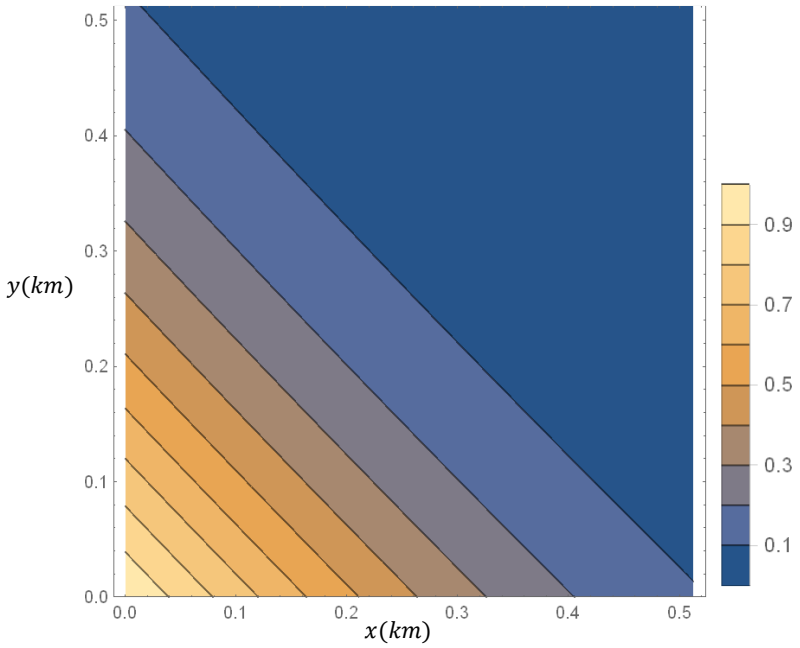

Figure 1b. Contour graph for the concentration profiles obtained from Eq. (30) at time $t = 0.5\,(year)$ in the xy -plane.

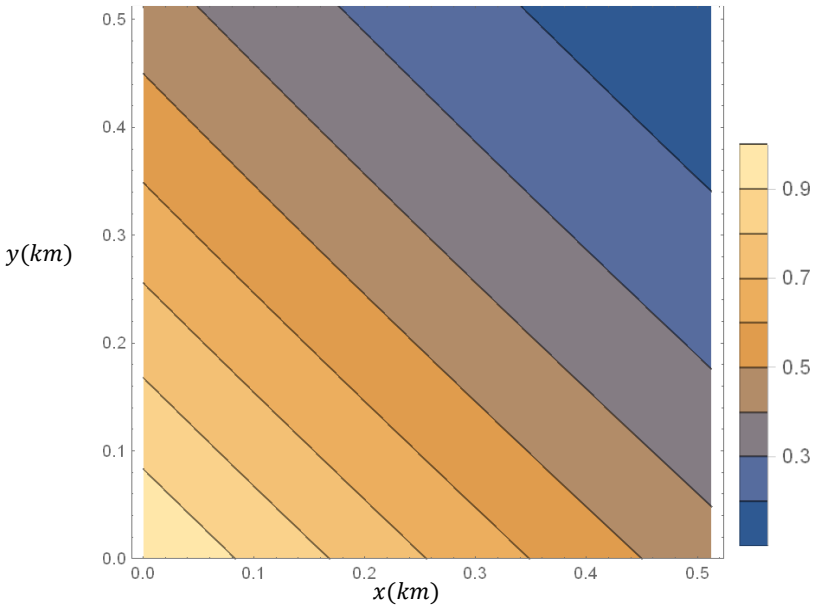

Figure 1c. Contour graph for the concentration profiles obtained from Eq. (30) at time $t = 2.0\,(year)$ in xy -plane.

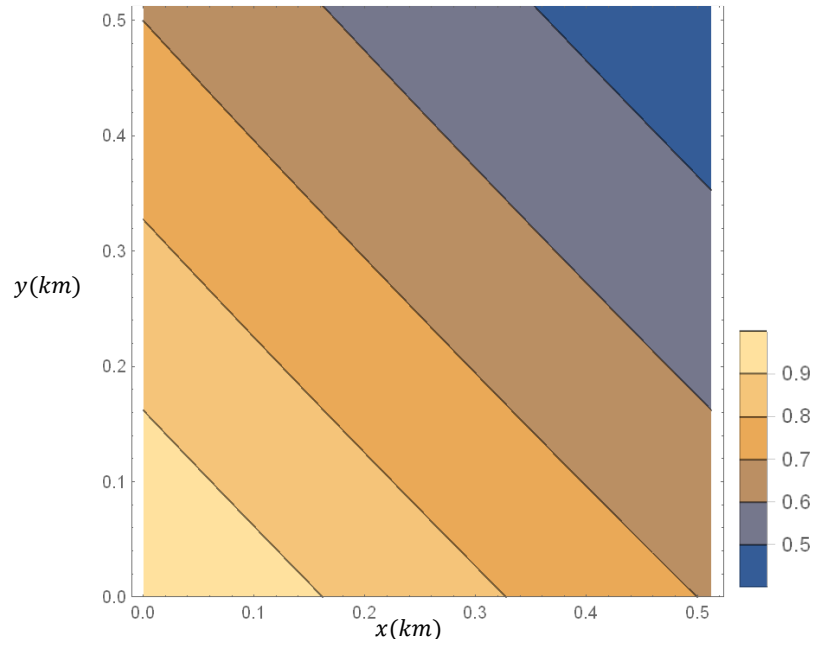

Figure 1d. Contour graph for the concentration profiles obtained from Eq. (30) at time $t = 5.5\,(year)$ in xy -plane.

Figs.1b, 1c and 1d explore the concentration profiles at different times $t = 0.5,\ 2.0, 5.5\,(year)$ respectively. All these three times are taken from time domain $0 < t\,(year) \le 1$, $1 < t\,(year) \le 5$ and $t\,(year) > 5$, respectively. This means that all three figures (Figs.1b, 1c and 1d) together represent the concentration distribution of Fig. 1a in different ways. Figs. 1b, 1c and 1d show that the concentration level in the domain increases with time inside the domain. The concentration level on the x-axis is greater than the concentration level on the y-axis for same radial distances from origin. This is because the longitudinal components of the diffusion coefficient and groundwater velocity are larger than the transverse components, which is consistent with the established theory [24].

As we move from the x-axis to the y-axis, keeping the radial distance constant, the level of the solute concentration decreases with time.

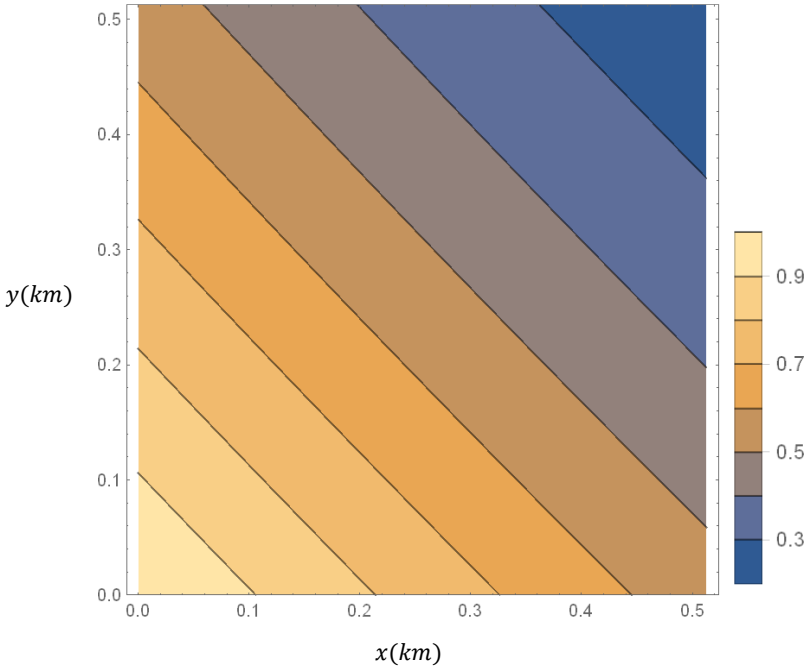

Figure 2a. Contour graph for the concentration profiles obtained from Eq. (30) for various dispersion coefficients $D_{xx0} = 0.06\ \left(km^2\, year^{-1}\right)$, $D_{yy0} = 0.04\ \left(km^2\, year^{-1}\right)$ and $D_{xy0} = 0.0053\ \left(km^2\, year^{-1}\right)$ in xy -plane.

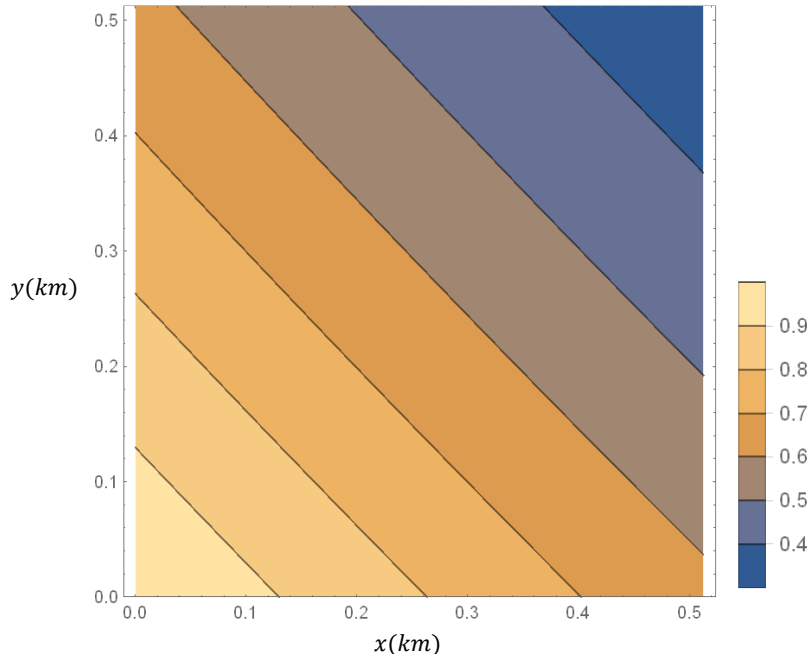

Figure 2b. Contour graph for the concentration profiles obtained from Eq. (30) for various dispersion coefficients $D_{xx0} = 0.09\ \left(km^2\, year^{-1}\right)$, $D_{yy0} = 0.07\ \left(km^2\, year^{-1}\right)$ and $D_{xy0} = 0.0083\ \left(km^2\, year^{-1}\right)$ in xy -plane.

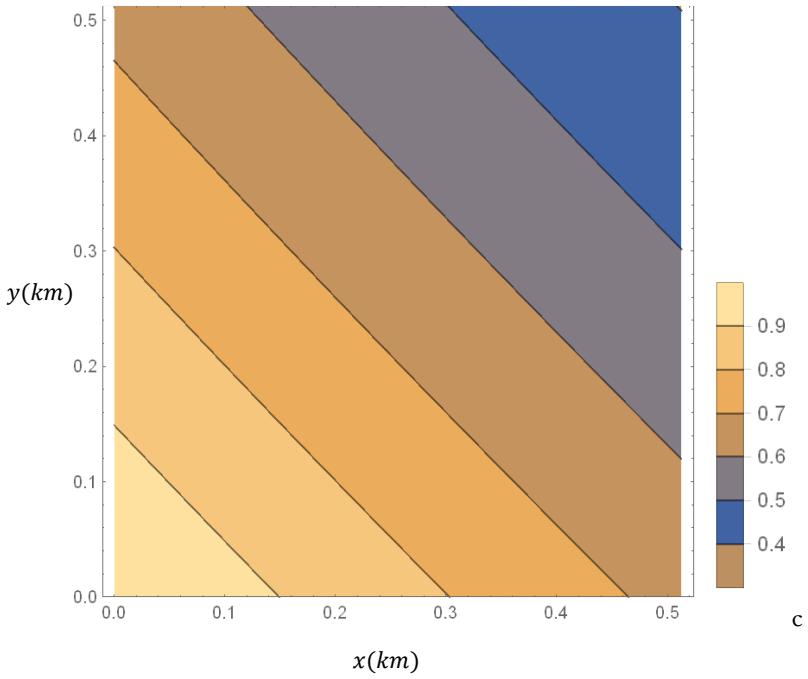

Figure 2c. Contour graph for the concentration profiles obtained from Eq. (30) for different dispersion coefficients $D_{xx0} = 0.12\left(km^2\,year^{-1}\right)$, $D_{yy0} = 0.10\left(km^2\,year^{-1}\right)$ and $D_{xy0} = 0.0113\left(km^2\,year^{-1}\right)$ in xy -plane.

In Figs. 2a, 2b, and 2c, the concentration distribution patterns are represented at time $t = 2.0\left(year\right)$ by contour plots for three different dispersion coefficients in the time domain $1 < t\left(year\right) \leq 5$ time and fixed heterogeneity parameters $a = 0.1\left(km^{-1}\right)$ and $b = 0.1\left(km^{-1}\right)$. The dispersion in corresponding components increases from Fig.2a to Fig.2c. Inside the region, as the dispersion coefficient increases, the concentration level over the entire domain also increases. The rate of change in the concentration level may be different in different directions. For example, concentration changes more rapidly along the y-axis than along the x-axis. Therefore, it can be concluded that dispersion plays an important role in the solute transport phenomenon.

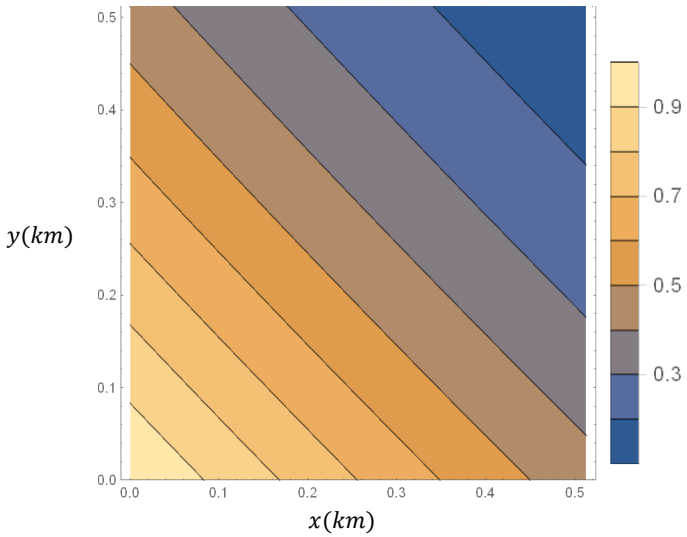

Figure 3a. Contour graph for the concentration profiles obtained from Eq. (30) for heterogeneity parameters $a = 0.1\left(km^{-1}\right)$ and $b = 0.1\left(km^{-1}\right)$ in xy -plane.

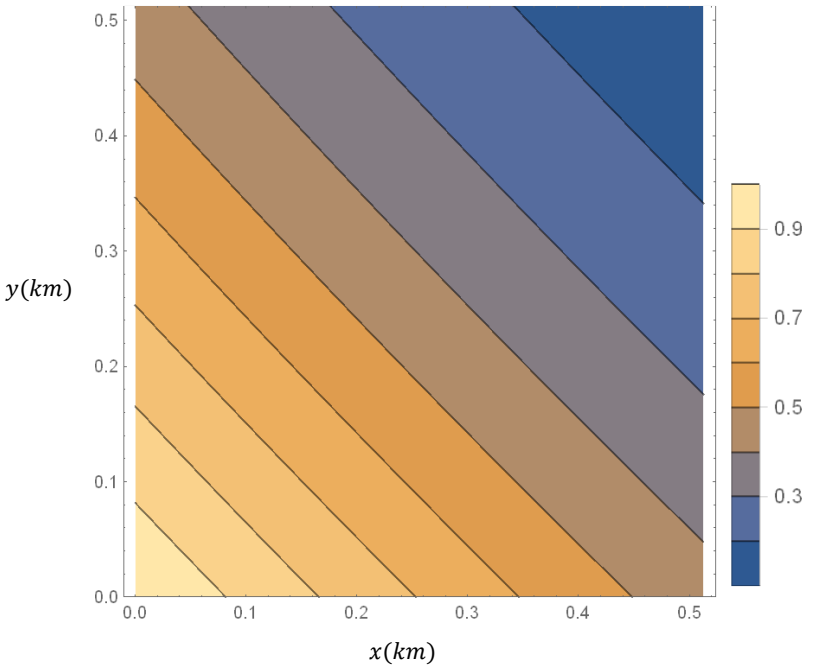

Figure 3b. Contour graph for concentration profiles obtained from Eq. (30) for heterogeneity parameters $a = 0.15\left(km^{-1}\right)$ and $b = 0.15\left(km^{-1}\right)$ in xy -plane.

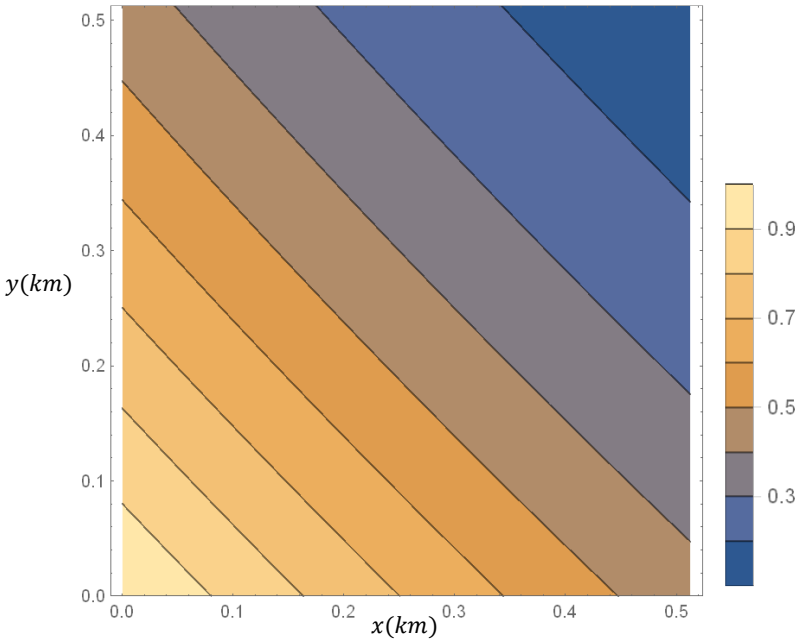

Figure 3c. Contour graph for concentration profile obtained from Eq. (30) time $t = 2.0(year)$ and heterogeneity parameters $a = 0.2\left(km^{-1}\right)$ and $b = 0.2\left(km^{-1}\right)$ in xy -plane.

In Figs.3a, 3b, and 3c, the concentration distribution patterns along with the contour plots represent at time $t = 2.0\left(year\right)$ in the time domain $1 < t\left(year\right) \leq 5$ and for fixed dispersion coefficients $D_{xx0} = 0.12\left(km^2\,year^{-1}\right)$, $D_{yy0} = 0.10\left(km^2\,year^{-1}\right)$ and $D_{xy0} = 0.0113\left(km^2\,year^{-1}\right)$ for three sets of heterogeneity parameters 'a' and 'b'. The dispersion and groundwater velocity

increase with an increase in the heterogeneity parameters at a certain point and consequently the solute is bounded to move more rapidly. Hence concentration slows down at that point. Furthermore, it is concluded that the concentration decreases faster along the y-axis than along the x-axis.

Case II: For Finite Porous Domain

Figs. 4a, 4b, 4c, and 4d are drawn for finite porous medium. Fig.4a is the surface graph in xy -plane while Figs. 4b, 4c, and 4d are contour graphs drawn for three different times $t = 0.5,\ 2.0,5.5\,(year)$, respectively and for dispersion coefficients $D_{xx0} = 0.06\ (km^2\,year^{-1}), D_{yy0} = 0.04\ (km^2\,year^{-1}),\ D_{xy0} = 0.0053\ (km^2\,year^{-1})$ and for heterogeneity parameter $a = 0.1(km^{-1})$ and $b = 0.1(km^{-1})$ for all these graphs (Figs. 4a, 4b, 4c, and 4d).

Fig.4a explores the concentration profiles at different times $t = 0.5\,(year),\ t = 2.0\,(year)$ and $t = 5.5\,(year)$ Concentration levels are increase with time within the domains, as groundwater velocity and dispersion coefficients varies with time across all time domains, as shown in Eq. (45). The non-source concentration is affected by the concentration introduced at the source end after a given time in a finite domain, while the concentration introduced at the source end has no effect on the non-source end in the semi-infinite domain.

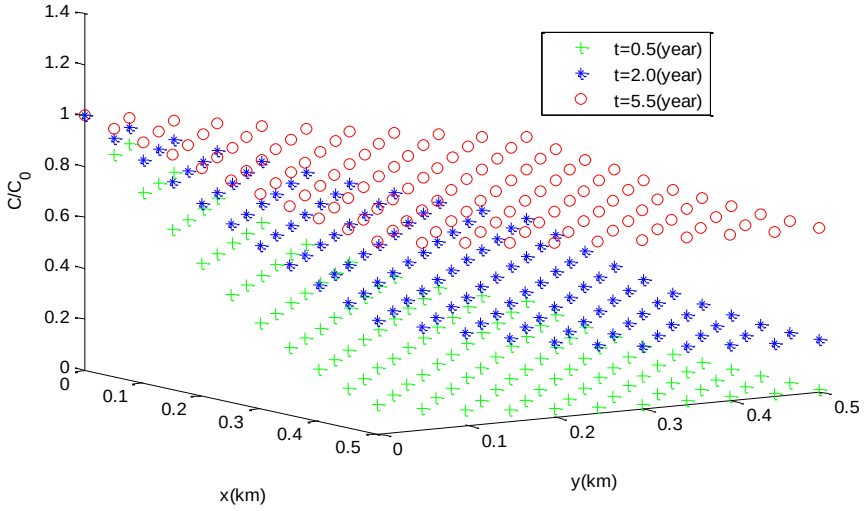

Figure 4a. Surface graph for the concentration profiles obtained from Eq. (44) in three different times period $t = 0.5\,(year)$, $t = 2.0\,(year)$ and $t = 5.5\,(year)$.

In the first two time domains, the dispersion coefficient and groundwater velocity increase with time and the result is that the concentration increases more slowly in the first domain than in the second, as in the semi-infinite domain. On the other hand, in the last time domain, the concentration value increases asymptomatically. In contrast to previous studies, the dispersion coefficient follows different patterns at different time intervals because the dispersion depends on the groundwater velocity which can vary with time.

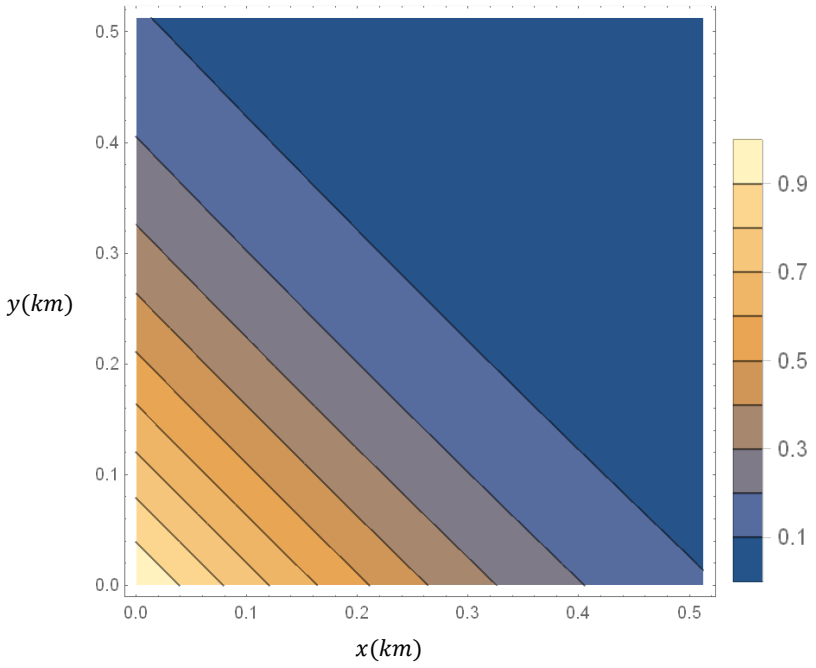

Figure 4b. Contour graph for the concentration profiles obtained from Eq. (44) at time $t = 0.5\,(year)$ in xy -plane.

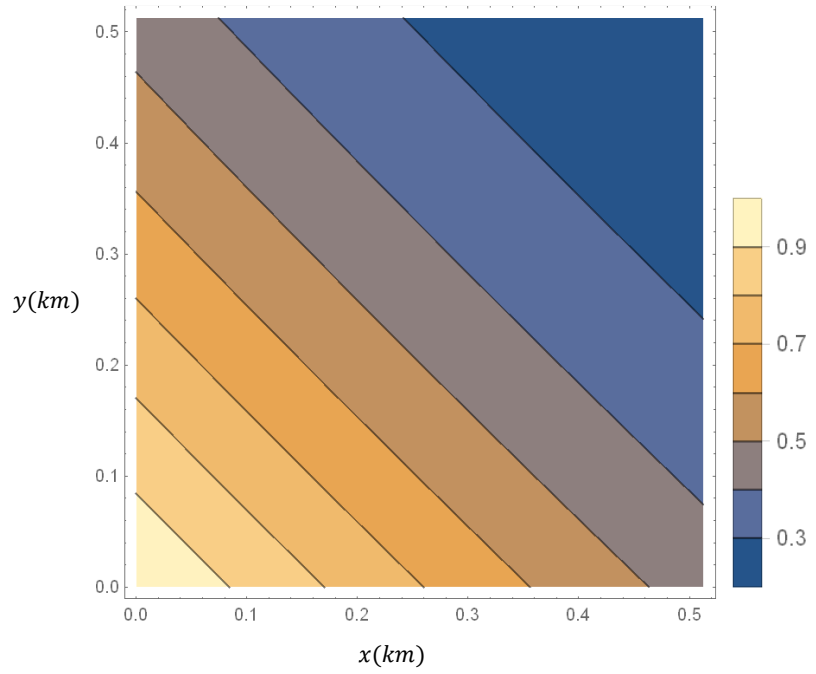

Figure 4c. Contour graph for the concentration profiles obtained from Eq. (44) at time $t = 2.0\,(year)$ in xy -plane.

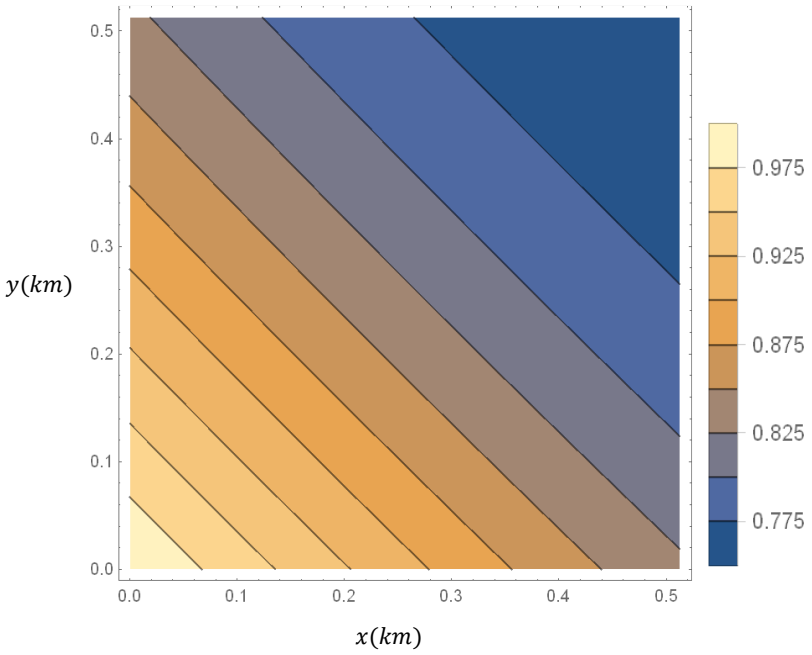

Figure 4d. Contour graph for the concentration profiles obtained from Eq. (44) at time $t = 5.5\,(year)$ in xy plane.

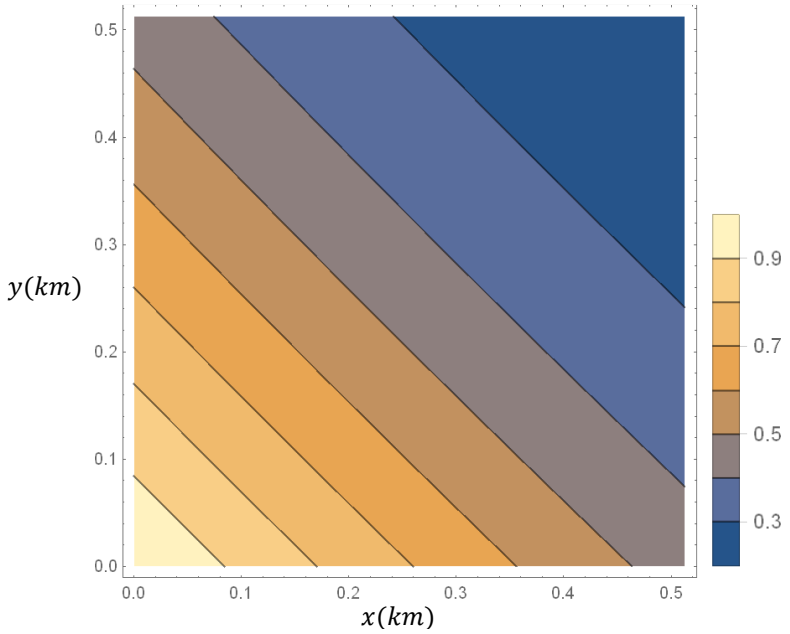

Figure 5a. Contour graph for the concentration profiles obtained from Eq. (44) for various dispersion coefficients $D_{xx0} = 0.06\,(km^2\,year^{-1}), D_{yy0} = 0.04\,(km^2\,year^{-1})$ and $D_{xy0} = 0.0053\,(km^2\,year^{-1})$ in xy -plane.

Figs.4b, 4c and 4d explore the concentration profiles with contour plot view for different times $t = 0.5,\ 2.0, 5.5\,(year)$ in time domain $0 < t\,(year) \le 1$, $1 < t\,(year) \le 5$ and $t\,(year) > 5$, respectively, in square space domain $0 < x\,(km) \le 0.512, 0 < y\,(km) \le 0.512$. It means all these three figures together represent the concentration profile of Fig. 4a. with different approach. Concentration level rises up at each area of square region inside the region from Fig.4b to Fig.4d i.e., with time. At equal distances from the beginning point on x-axis and y axis, the concentration level on x-axis is higher than that of on

y-axis. Such is the case here because the x-axis component of dispersion and groundwater velocity (longitudinal components) is greater than that of y-axis component (lateral/transversal components). Therefore, spreading solute decreases for fixed time on moving from x-axis to y-axis keeping radial distance fixed.

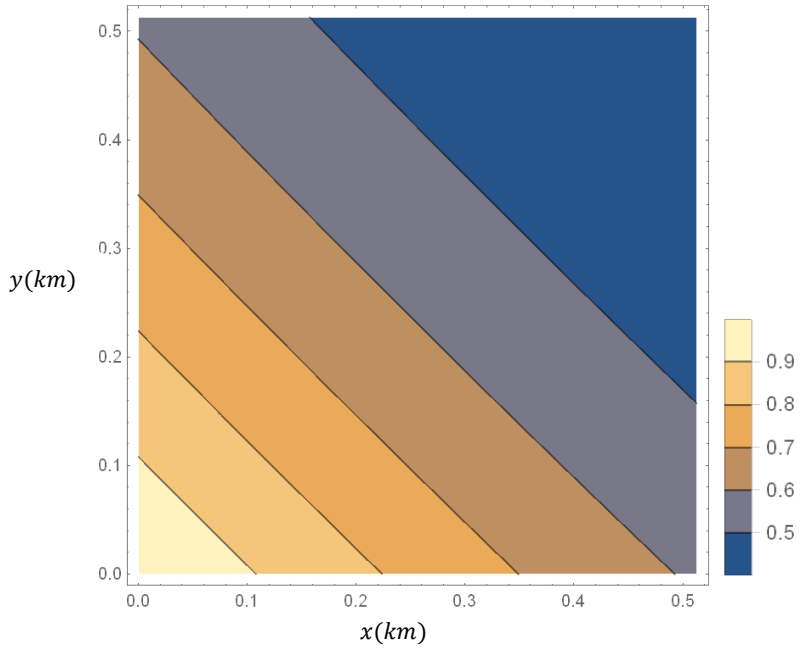

Figure 5b. Contour graph for the concentration profiles obtained from Eq. (44) for various dispersion coefficients $D_{xx0} = 0.09\ \left(km^2\, year^{-1}\right)$, $D_{yy0} = 0.07\ \left(km^2\, year^{-1}\right)$ and $D_{xy0} = 0.0083\ \left(km^2\, year^{-1}\right)$ in xy -plane.

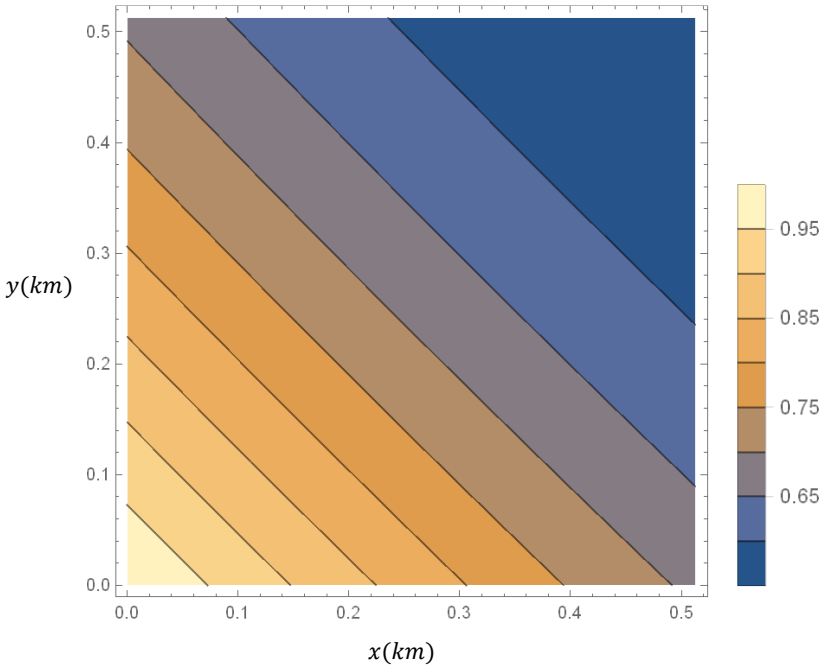

Figure 5c. Contour graph for the concentration profiles obtained from Eq. (44) for various dispersion coefficients $D_{xx0} = 0.12\ \left(km^2\, year^{-1}\right)$, $D_{yy0} = 0.10\ \left(km^2\, year^{-1}\right)$ and $D_{xy0} = 0.0113\ \left(km^2\, year^{-1}\right)$ in xy -plane.

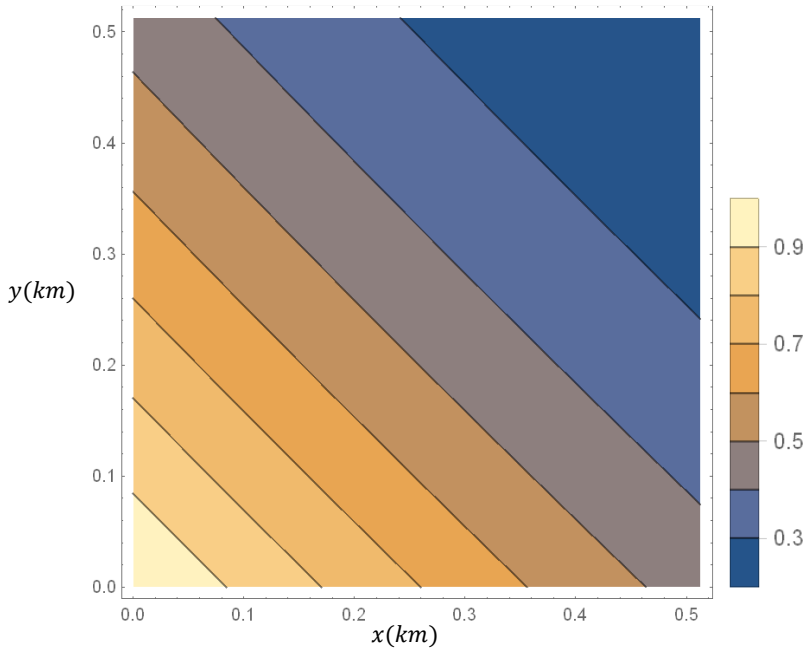

Figure 6a. Contour graph for the concentration profiles obtained from Eq. (44) for heterogeneity parameters $a = 0.1\left(km^{-1}\right)$ and $b = 0.1\left(km^{-1}\right)$ in xy -plane.

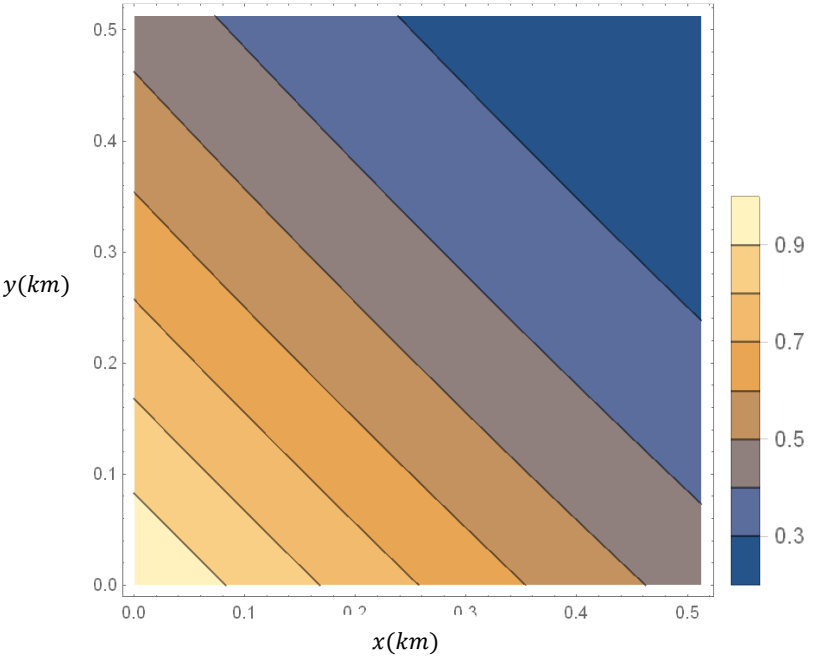

Figure 6b. Contour graph for the concentration profiles obtained from Eq. (44) for heterogeneity parameters $a = 0.15\left(km^{-1}\right)$ and $b = 0.15\left(km^{-1}\right)$ in xy -plane.

The concentration distribution patterns in Figures 5a, 5b, and 5c demonstrate the effect of three sets of dispersion coefficients in the time domain at $t = 2.0(year)$ at time and fixed heterogeneity parameter $a = 0.1\left(km^{-1}\right)$ and $b = 0.1\left(km^{-1}\right)$.The dispersion in

corresponding components increases from Fig.5a to Fig.5c. Furthermore, as the dispersion coefficient increases, the concentration level also increases at every point in the domain except the starting point. The rate of change in concentration levels may vary in directions. As can be seen, the concentration changes faster along the y-axis than on the x-axis. Therefore, it can be concluded that dispersion plays an important role in the solute transport phenomenon.

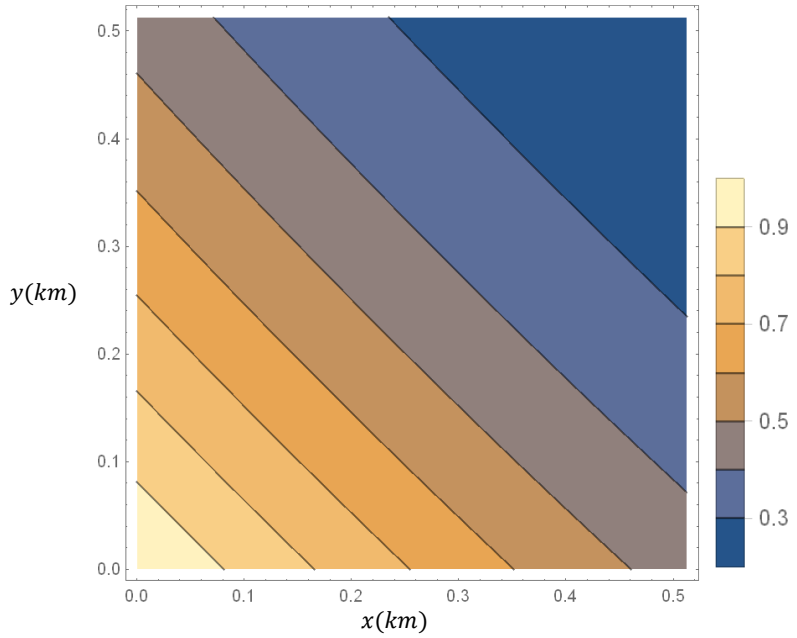

Figure 6c. Contour graph for the concentration profiles obtained from Eq. (44) for heterogeneity parameters $a = 0.2\left(km^{-1}\right)$ and $b = 0.2\left(km^{-1}\right)$ in xy -plane.

Figs.6a, 6b and 6c show the concentration distribution patterns at time $t = 2.0\left(year\right)$ in time domain $1 < t\left(year\right) \leq 5$ and for fixed dispersion coefficients $D_{xx0} = 0.12\left(\mathrm{km}^2\,\mathrm{year}^{-1}\right), D_{yy0} = 0.10\left(km^2\,year^{-1}\right)$ and $D_{xy0} = 0.0113\left(km^2\,year^{-1}\right)$ through a contour graph for the three heterogeneity parameters 'a' and 'b'. It can be inferred that as the value of the heterogeneity parameter at a location increases, the dispersion and groundwater velocity at that point also increase. Hence, the solute is eventually forced to move faster. Thereafter, the concentration slows down at this particular point. Furthermore, the contour plot shows that the concentration decreases faster along the y-axis than along the x-axis.

As can be seen from Figs (2a and 5a), (2b and 5b), (2c and 5c), (3a and 6a), (3b and 6b) and (3c and 6c), the concentration level at a certain point in the finite domain is higher than the semi-infinite domain. Furthermore, it was observed that the concentration level increases more rapidly along the transverse direction (y-axis) than longitudinal direction (x-axis).

4. Conclusions

Analytical solutions for two-dimensional conservative solute transport in a heterogeneous porous medium with degenerate forms of groundwater velocity and dispersion are obtained using Laplace Integral Transform Technique. The effects of the dispersion coefficient and groundwater velocity are supposed to be time and space-dependent. Keeping all parameter values the same for the posed problem, the concentration profiles in finite and semi-infinite porous media are demonstrated. Different diagrams are used to describe the solute concentration distribution. The developed model may help policy makers in water management to objectively assess pollution levels at a given time and position. This study is also important for analyzing the validity of numerical solutions.

References

[1] Hoopes, J.A., Harleman, D.R.F. (1965). Waste water recharge and dispersion in porous media, Technical Report No. 75

[2] Bruce, J.C., Street, R.L. (1966). Studies of Free Surface Flow and Two-Dimensional Dispersion in Porous Media. Civil Eng. Dept. Stanford Uni., Stanford California. Report No. 63.

[3] Wang, H.F., Anderson, M.P. (1982). Introduction to groundwater modeling. Finite difference and finite element methods. Freeman and Co, San Diego, 237.

[4] Fetter, C.W. (2001). Applied hydrogeology. Prentice Hall Inc.; New Jersey.

[5] Goode, D.J., Konikow L.F. (1990). Apparent dispersion in transient groundwater flow. Water Resources Research; 26(10): 2339–2351.

[6] Batu, V. (1993). A generalized two-dimensional analytical solute transport model in bounded media for flux-type finite multiple sources. Water Resources Research; 29(8):2881–2892.

[7] Batu, V. (1989). A generalized two-dimensional analytical solution for hydrodynamic dispersion in bounded media with the first-type boundary condition at the source. Water Resources Research; 25(6): 1125–1132.

[8] Smith, R. E., Smettem, K. R. J., Broadbridge, P. and Woolhiser., D. A. (2002). Infiltration theory for hydrologic applications. American Geophysical Union.

[9] Chen, J. S., Ni CF, Liang C. P. (2008). Analytical power series solutions to the two-dimensional advection-dispersion equation with distance-dependent dispersivities. Hydrological Processes; 22(24):4670-4678.

[10] Yadav, R. R., Jaiswal, D. K., Gulrana. (2011). Two-dimensional solute transport for periodic flow in isotropic porous media: an analytical solution hydrological processes Hydrol. Process. Published online in Wiley Online Library (wileyonlinelibrary.com), 26(22):3425-3433, DOI: 10.1002/hyp.8398.

[11] Jaiswal, D. K., Kumar A. and Yadav R. R. (2012). Unsteady Dispersion in Two-Dimensional Homogeneous Porous Media. International Conference on Modeling and Simulation of Diffusive Processes and Applications; 75.

[12] Singh, M. K., Mahato, N. K. (2012). Two Dimensional Solute Transport for Temporally Dependent Source Concentration in Semi-Infinite Aquifer. International Conference on Modeling and Simulation of Diffusive Processes and Applications.

[13] Singh, P., Yadav S. K., Perig A. V. (2012). Two –Dimensional Solute Transport from a Varying Pulse - Type Point Source along Exponentially Varying Unsteady Flow through Heterogeneous Medium. International Conference on Modeling and Simulation of Diffusive Processes and Applications; 68.

[14] Singh, M. K., Ahamad S. (2012). One-dimensional Non-reactive Solute Transport in a Semi-infinite Aquifer Subject to a Temporally Dependent Dispersion with Temporally Dependent Input Concentration. International Conference on Modeling and Simulation of Diffusive Processes and Applications.

[15] Perez Guerrero, J. S., Pimentel L. C. G., Skaggs T. H., Van Genuchten, M. th. (2009). Analytical solution of the advection-diffusion transport equation using a change-of-variable and integral transform technique. International Journal of heat and Mass Transfer; 52:3297-3304.

[16] lizadeh, R., Beaudoin, J. J., Raki, L., (2010). Viscoelastic nature of calcium silicate hydrate. Cement and Concrete Composites; 32(5):369-376.

[17] De Dreuzy, J. R., Beaudoin, A., Erhel, J. (2007). Asymptotic dispersion in 2D heterogeneous porous media determined by parallel numerical simulations. Water Resour. Res.; 43:W10439, doi:10.1029/2006WR005394

[18] Chen, J. S. (2007). Two-dimensional power series solution for non axisymmetrical transport in a radially convergent tracer test with scale-dependent dispersion. Adv. Water Resour; 30(3):430-438.

[19] Singh, M. K., Singh, P., Singh V. P. (2010). Analytical solution for Two-Dimensional Solute Transport in Finite Aquifer with Time-Dependent Source Concentration Journal of Engineering Mechanics; 136(10) 1309-1315.

[20] Chen, J. S., Chen, J. T, Liu C.W., Liang C. P., Lin C. W. (2011). Analytical solutions to two dimensional advection-dispersion equation in cylindrical coordinate in finite domain subject to first-and third-type inlet boundary conditions. Journal of Hydrology; 405(3-4) 522-531.

[21] Zheng, C., Bennett, G. D. (1995). Applied Contaminant Transport Modelling: Theory and Practice. Van Nostrand Reinhold (John Wiley and Sons), New York.

[22] Crank, J., Gupta, R. S. (1975). Isotherm migration method in two dimensions. International Journal of Heat and Mass Transfer; 18(9):1101-1107.

[23] Kumar, A., Jaiswal D. K., Kumar, N. (2010). Analytical solutions to one-dimensional advection–diffusion equation with variable coefficients in semi-infinite media. Journal of Hydrology; 380:330-337.

[24] Cirpka, O.A., Frind, E.O., Helmig, R. (1999). Numerical simulation of biodegradation controlled by transverse mixing. J. Contam. Hydrol; 40 (2):159-182.